The influence of direct air-cooled units on primary frequency regulation in power systems

Yufeng Guo [1*], Dongrui Zhang [1], Jie Wan [2], Daren Yu [2]

[1] School of Electrical Engineering and Automation, Harbin Institute of Technology, Harbin, China
[2] School of Energy Science and Engineering, Harbin Institute of Technology, Harbin, China
[*] guoyufenghit@163.com

Abstract: Performance of air-cooled units is significantly affected by meteorological conditions because they use the ambient air directly as the cooling medium. The purpose of this study is to determine the influence of air-cooled units on grid stability under extreme meteorological conditions. Based on the characteristics of air-cooled units, cooling air face velocity and temperature are two main meteorological factors taken into consideration. A dynamic model of the air-cooled units is developed. Since grid frequency is a representation of grid stability, the above model is then applied to a mathematical model to analyse the primary frequency regulation process of a grid. A coefficient to measure the primary frequency regulation ability (PFRA) is defined and the calculation of PFRA is put forward. To increase the reliability of the study, performance of the grid under different meteorological conditions is also studied in frequency domain. Case studies under generator tripping and steep load rising conditions are studied. The corresponding PFRA and the maximum capacity proportion of air-cooled units are calculated. This study provides a constructive guide for the operation of air-cooled units under different meteorological conditions.

1. Introduction

Water is a precious resource on earth. There are some regions which are scarce in water resources while abundant in coal reservation, like the south-western China [1]. In these regions, power plants use coal as the main energy source. Construction of air-cooled units develops rapidly in these areas because they can save water consumption, as they take the ambient air directly as the cooling medium. These years, air-cooled units constructed in China have developed into 600MW and 1000MW ones. China is gradually becoming a country with the world's greatest installed capacity of air-cooled units. The progress of air-cooled units is having a more and more significant impact on regional power system.

The major difference between traditional water-cooled units and air-cooled units is the heat exchange medium [2,3]. Different from water-cooled units, which use water, air-cooled units take the ambient air directly as the cooling medium. The heat-transfer process between the ambient air and steam is a primary surface heat-transfer process. This makes the performance of air-cooled units greatly affected by meteorological conditions, such as cooling air face velocity and temperature [4-6].

Several studies demonstrate that air-cooled systems are strongly affected by meteorological conditions. In [7], mathematical model of a direct air-cooled condenser is made and its performance under different disturbances are analysed. In [1], mathematical model of the cold-end system of an air-cooled

unit is put forward, and a cold-end adjustment system is designed to reduce the fluctuations of the backpressure caused by meteorological fluctuations. The performance of gas turbines with vapour absorption inlet air cooling system under different meteorological conditions is studied in [5], and it has been observed that the plant efficiency reduces with the increase in ambient temperature.

From previous works, real-time power generated by an air-cooled unit is fluctuant when the meteorological conditions change [8-10]. As the capacity proportion of air-cooled units increases, the instability of air-cooled units would also cause disturbances in grid stability. In this study, grid frequency is considered as a representation of grid stability [11,12].

Frequency regulation of the grid is a well-studied topic with significant research works. A stable grid frqequency depends on the balance of power generations and power consumptions [13-15]. In [16], a frequency response analysis approach considering the effect of emergency control/protection schemes is included. In [17], boundaries of power system frequency regulation abilities are defined and the mathematical model of a three-area power system is established.

To the best of the authors' knowledge, few studies have been published on the influence of direct air-cooled units on the stability of power systems. Given all this, a quantitative study of the impact of air-cooled units on the stability of a regional power grid is needed. Thus, the primary frequency regulation process of the grid is analysed here.

This paper is organized as follows: Section 2 proposes the mathematical model of air-cooled units and a regional grid model for frequency analysis. In Section 3, a coefficient to measure the primary frequency regulation ability of the grid is defined and the calculation of PFRA is given. Case studies are presented in Section 4. Finally, conclusions are presented in Section 5.

2. Mathematical modelling

2.1. Mathematical model of an air-cooled condenser

Fig.1 shows the basic structure of the steam-water system of an air-cooled unit [18-22]. An air-cooled unit and a regular water-cooled unit are generally consistent in their structures. The major difference is in their cold-end systems. The cold-end system of an air-cooled unit consists of an air-cooled condenser, an axial cooling fan, and a vertical engine, while a water-cooled unit uses the cooling tower as its major component to cool the exhaust steam. In an air-cooled unit, steam flows through the air-cooled condenser and gets cooled by the air flow generated by the axial cooling fan, which is a primary surface heat-transfer process.

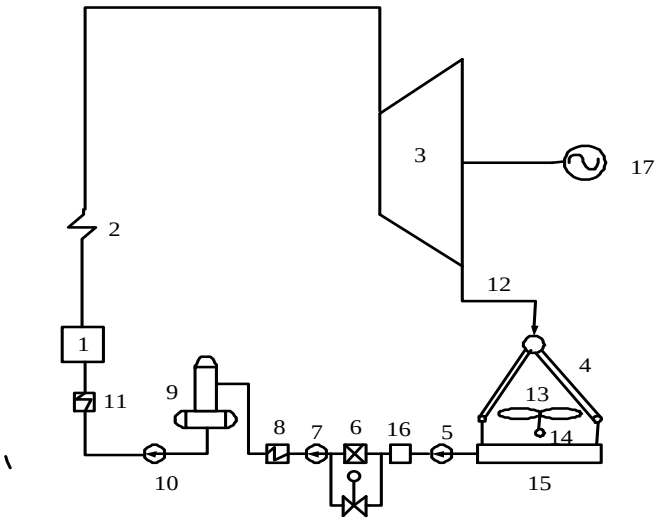

Fig. 1. *Basic structure of the steam-water system of an air-cooled unit*
1-boiler 2-superheater 3-turbine 4-air-cooled condenser 5-condensate pump 6-condensing water treatment system 7-condensing water booster pump 8-low pressure heater 9-deaerator 10-feed pump 11-high pressure heater 12-turbine exhaust pipe 13-axial cooling fans 14-vertical motor 15-condensate tank 16-iron remover 17-generator

Output of an air-cooled unit is related to the backpressure of its condenser. With lower backpressure, power generated by the unit could be increased [1]. Backpressure of the condenser in an air-cooled unit is affected by many factors, such as the ambient air temperature. The backpressure usually ranges from 5kpa to 60kpa.

Here the steam flowing into the condenser is assumed to be equal to that flowing out of the condenser. According to the continuity of steam flow, the product of the saturated steam density ρ and the volume of the condenser V is equal to the difference between the steam flow into the condenser q_{in} and the flow of the condensed steam q_{n}, which can be expressed as:

$$V\frac{d\rho}{dt}=q_{\text{in}}-q_{\text{n}} \tag{1}$$

Q_{k} represents the heat absorbed by the cooling air, which can be calculated as:

$$Q_{\text{k}}=A\upsilon\rho_{\text{a}}c_{\text{a}}(1-\exp(-\alpha_{\text{NTU}}))(t_{\text{s}}-t_{\text{a}}) \tag{2}$$

where $A\left(\text{m}^2\right)$ is the windward area of the air-cooled condenser; $\upsilon\left(\text{m/s}\right)$ is the cooling air face velocity; ρ_{a} is the average density of air, which is $1.17\,\text{kg/m}^3$; c_{a} is the coefficient of specific air capacity at constant pressure, which is $1000\,\text{J/(kg}\cdot\text{K)}$; $t_{\text{s}}\left(\text{K}\right)$ is the steam saturation temperature; $t_{\text{a}}\left(\text{K}\right)$ is the ambient air temperature; α_{NTU} is the heat transfer ratio, which can be expressed as:

$$\alpha_{\mathrm{NTU}}=\frac{k_0 A_{\mathrm{S}}}{\rho_{\mathrm{a}} \upsilon A c_{\mathrm{a}}}=\frac{k_0 z}{\rho_{\mathrm{a}} \upsilon c_{\mathrm{a}}} \tag{3}$$

where:

$$k_0=m(0.31833 v^3-3.6969 v^2+14.832 v+15.691) \tag{4}$$

where $A_{\mathrm{S}}\left(\mathrm{m}^2\right)$ is the heat exchange area of the radiator; z is the ratio of total heat transfer area to windward area, which is dimensionless [23]; $k_0\left(\mathrm{W/(m^2 \cdot K)}\right)$ is the total heat transfer coefficient; m is the proportion of finned area of the air-cooled radiator, which is dimensionless.

In condensing zone, steam temperature is the same as saturation temperature and assumes to remain constant. Therefore, the saturation temperature is taken as the average temperature of steam. Based on the dynamic balance equation of heat transfer, the heat exchange process can be expressed as:

$$c_{\mathrm{s}} m_{\mathrm{s}} \frac{d t_{\mathrm{s}}}{d t}=r q_{\mathrm{n}}-A \upsilon \rho_{\mathrm{a}} c_{\mathrm{a}}\left(1-\exp\left(-\alpha_{\mathrm{NTU}}\right)\right)\left(t_{\mathrm{s}}-t_{\mathrm{a}}\right) \tag{5}$$

where c_{s} is the coefficient of specific steam capacity at constant pressure, which is taken as $1853.5\mathrm{J/(kg \cdot K)}$; $m_{\mathrm{s}}\left(\mathrm{kg}\right)$ is the mass of steam in the condenser; $r\left(\mathrm{J/kg}\right)$ is the latent heat of vaporization for saturated steam.

From equation (5), q_{n} can be calculated by:

$$q_{\mathrm{n}}=\frac{c_{\mathrm{s}} m_{\mathrm{s}} \frac{d t_{\mathrm{s}}}{d t}+A \upsilon \rho_{\mathrm{a}} \mathrm{c}_{\mathrm{a}}\left(1-\exp\left(-\alpha_{\mathrm{NTU}}\right)\right)\left(t_{\mathrm{s}}-t_{\mathrm{a}}\right)}{r} \tag{6}$$

The status change process of steam in the condenser is assumed to be a polytropic process.

Thus, the relation between the backpressure and the saturated steam density is given by:

$$P_{\mathrm{c}} / \rho^n=c \tag{7}$$

$$\ln P_{\mathrm{c}}-n \ln \rho=c \tag{8}$$

where c is a constant; n is a polytropic constant that is normally taken as 1.3; $P_{\mathrm{c}}\left(\mathrm{Pa}\right)$ is the backpressure of the condenser.

Through derivation, equation (8) can be expressed as:

$$\frac{\mathrm{d} \rho}{\mathrm{d} t}=\frac{\rho}{n P_{\mathrm{c}}} \frac{\mathrm{d} P_{\mathrm{c}}}{\mathrm{d} t} \tag{9}$$

By substituting equation (6) and (9) into equation (1), $\frac{\mathrm{d}P_{\mathrm{c}}}{\mathrm{d}t}$ can be calculated by:

$$\frac{dP_c}{dt} = (q_{in} - rq_n) / \left(\frac{rV\rho}{nP_c} \right) \tag{10}$$

According to the thermodynamic properties of saturated water and saturated steam, r and t_s would change as P_c changes. By curve fitting, the relation can be identified as follows:

$$t_s = a_3 \log^3(P_c) + a_2 \log^2(P_c) + a_1 \log(P_c) + a_0 \tag{11}$$

where a_0, a_1, a_2, a_3 are constants.

Through derivation, equation (11) can be expressed as:

$$\frac{dt_s}{dt} = [3a_3(\log P_c)^2 / P_c + 2a_2(\log P_c) / P_c + a_1(\log P_c) / P_c] \frac{dP_c}{dt} \tag{12}$$

The latent heat of vaporization is given by:

$$r = b_3 \log^3(1/P_c) + b_2 \log^2(1/P_c) + b_1 \log(1/P_c) + b_0 \tag{13}$$

where b_0, b_1, b_2, b_3 are constants.

Since

$$m_s = \rho V \tag{14}$$

The relationship between the steam density and the backpressure is expressed as the following fitted polynomial:

$$\rho = c_2 \cdot P_c^2 + c_1 \cdot P_c + c_0 \tag{15}$$

where c_0, c_1, c_2 are constants.

By substituting equation (12), (13) and (15) into equation (10), the derivative formula for the condenser's backpressure can be obtained. Calculations can be done with S-Function in MATLAB/Simulink. After integration, the backpressure in the condenser can be calculated.

In this paper, backpressure is approximately taken as the pressure of the condenser and the difference caused by the physical distance between air-cooled condenser and low pressure cylinder is ignored.

With application of thermodynamic charts for saturation water and steam and via MATLAB curve fitting function, the relation between steam enthalpy h_c and backpressure can be approximately worked out as:

$$h_c = d_1 \cdot P_c + d_0 \tag{16}$$

where d_0, d_1 are constants.

Fig. 2 shows the mathematical model of an air-cooled condenser. The input variables are the velocity of exhaust flowing from the low pressure cylinder, the ambient air temperature, and cooling air face velocity. The output variable is power of the low-pressure cylinder.

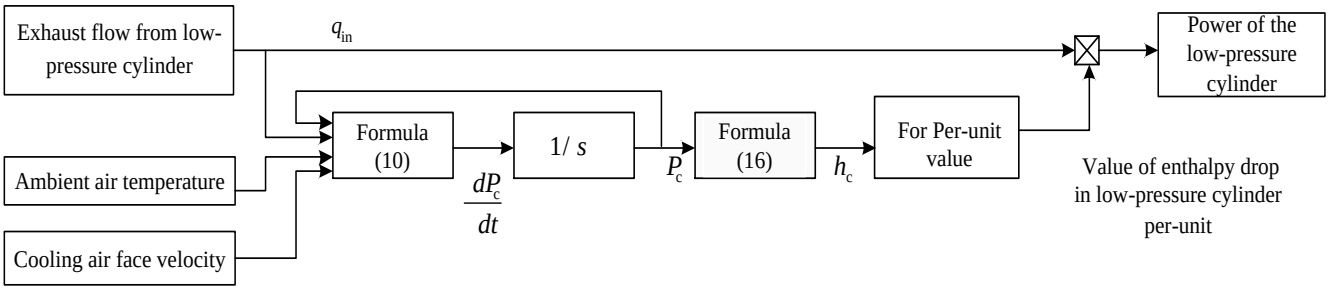

Fig. 2. *Model of an air-cooled condenser*

2.2. Mathematical model of an air-cooled unit

Based on the working principle of air-cooled condenser, mathematical model of a 600MW coal-fired reheating steam turbine is established, as shown in Fig. 3, where C_i is the coefficient of power quotient in each level of extraction flow; R_p is the speed droop coefficient of air-cooled unit; the input signal $R(s)$ is the pre-set load signal for air-cooled unit; and the output signal $\chi_{na}(s)$ is the rotating speed of air-cooled unit. $\chi_{NLa}(s)$ is the normalized value of load borne by air-cooled unit. The air-cooled condenser model in this part, which is marked by dotted lines, is the same as that in Fig.2.

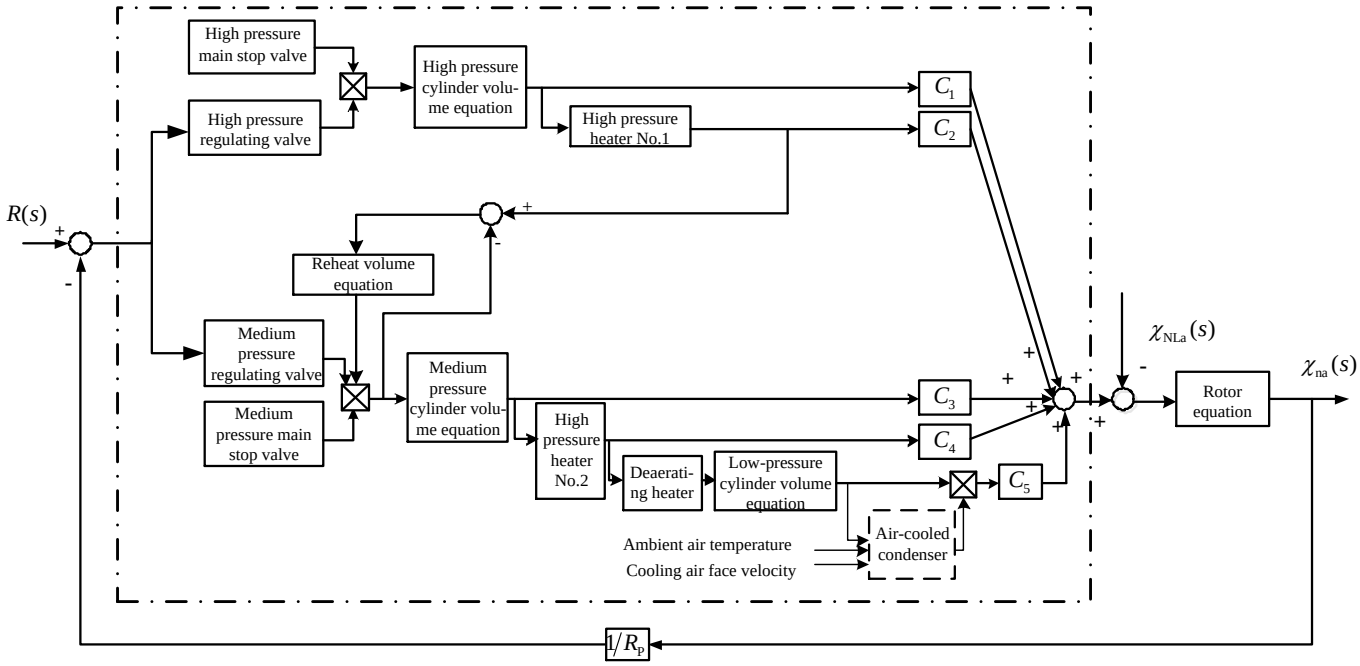

Fig. 3. *Model of a 600MW coal-fired reheating steam turbine with an air-cooled condenser*

2.3. Model of a regional power system including air-cooled units for frequency analysis

Fig.4 is the mathematical model of a grid with M synchronous generators running in parallel, where N_1 ($N_1 < M$) is the number of turbines performing in the secondary frequency regulation and N_2 ($N_2 < M$) is the number of turbines performing in primary frequency regulation [17]. $R_{\mathrm{P}i}$ is speed droop coefficient of generator i. α_i is the ratio of the installed capacity of generator i to the installed capacity of the whole power system. R_i is coefficient of power budget of the units that perform in the secondary frequency regulation, and $G_i(s)$ is the transfer function of a generator [24, 25]. $G_i(s)$ of air-cooled unit can be obtained by calculation and reduction of transfer functions included in the dash dot line square in Fig.3. Transfer functions of each component of the model in Fig.3 and values of the corresponding parameters are given in Table 1 and Table 2. Since the main stop valves are wide open when the unit is running, the transfer function for main stop valves is 1. Other examples of $G_i(s)$ are given in Table 3 [17]. $\chi_{\mathrm{NL}}(s)$ is normalized valued of load. By load characteristic modeling, we could get the data of $\chi_{\mathrm{NL1}}(s)$, $\chi_{\mathrm{NL2}}(s)$, and $\chi_{\mathrm{NL3}}(s)$ based on the data of $\chi_{\mathrm{NL}}(s)$. T is the control cycle of secondary frequency regulation, the value of which depends on the control mode of the grid. Values of all parameters are available at the dispatching centre. The output signal $\chi_{\mathrm{n}}(s)$ is the normalized value of frequency. $T_{\alpha i}$ is rotor time constant of generator i [24]. If there are M units in the electric power system, $T_{\alpha\Sigma}$ is the inertia time constant of electric power system, and β_Σ is load-frequency characteristic coefficient, where:

$$T_{\alpha\Sigma} = \sum_{i=1}^{M} \alpha_i T_{\mathrm{a}i} \tag{17}$$

$$\beta_\Sigma = \sum_{i=1}^{M} \alpha_i \beta_i \tag{18}$$

where β_i is the load-frequency characteristic coefficient of generator i.

Table 1 Transfer functions in Fig.3

Component	Transfer function
High cylinder volume equation	$\frac{1}{T_{\mathrm{cv1}}s+1}$
Medium cylinder volume equation	$\frac{1}{T_{\mathrm{cv2}}s+1}$

Low cylinder volume equation	$\frac{1}{T_{cv3}s+1}$
High-pressure regulating valve	$\frac{1}{(T_{hf1}s+1)T_{vh1}s}$
Medium-pressure regulating valve	$\frac{k_{pm}}{(T_{hf2}s+1)T_{vh2}s}$
Reheat volume equation	$\frac{1}{T_R s}$
Extraction check valve in high-pressure heater	$\frac{1}{(T_{chf1}s+1)T_{cq1}s+1}$
Extraction inertia loop in high-pressure heater	$\frac{1}{T_{r1}s+1}$
Extraction check valves in deaerating heater	$\frac{1}{(T_{chf2}s+1)T_{cq2}s+1}$
Extraction inertia loop in deaerating heater	$\frac{1}{T_{r2}s+1}$

Table 2 Parameter values of model in Fig.3

Parameters	Values
High-pressure cylinder volume time constant T_{cv1}	0.1279s
Medium-pressure cylinder volume time constant T_{cv2}	0.3051s
Low-pressure cylinder volume time constant T_{cv3}	0.1093s
Servo valve time constant in high-pressure regulating valve T_{hf1}	0.02s
Servo valve time constant in medium-pressure regulating valve T_{hf2}	0.02s
Hydraulic servo-motor time constant in high-pressure regulating valve T_{vh1}	0.2s
Hydraulic servo-motor time constant in medium-pressure regulating valve T_{vh2}	0.2s
Reheat volume time constant T_R	8.29s
Servo valve time constant of extraction check valve in high-pressure heater T_{chf1}	0.02s
Servo valve time constant of extraction check valve in deaerating heater T_{chf2}	0.02s
Hydraulic servo-motor time constant in extraction	0.92s

check valves in high-pressure heater T_{cq1}	
Hydraulic servo-motor time constant in extraction	0.92s
check valves in deaerating heater T_{cq2}	
Extraction inertia time constant in high-pressure	20s
heater T_{r1}	
Extraction inertia time constant in deaerating	30s
heater T_{r2}	
C_1	0.2149
C_2	0.0874
C_3	0.1471
C_4	0.1231
C_5	0.4275
k_{pm}	5
R_p	0.05

Table 3 Examples of $G_i(s)$ in Fig.4

Types	Transfer functions
Transfer function for hydro turbines	$G_i(s)=\frac{b_p(K_P+K_I/s+K_D s)}{b_p(K_P+K_I/s+K_D s)+1+(T_\sigma s+1)T_{ws}s}\cdot\frac{1-T_w s}{1+0.5T_w s}$
Transfer function for water-cooled condensing steam turbines	$G_i(s)=\frac{1}{T_{si}s+1}\cdot\frac{1}{T_{vi}s+1}$
Transfer function for water-cooled reheating steam turbines	$G_i(s)=\frac{1}{T_{sri}s+1}\cdot\frac{1}{T_{vri}s+1}\cdot\frac{\alpha_H T_{RHi}s+1}{T_{RHi}s+1}$

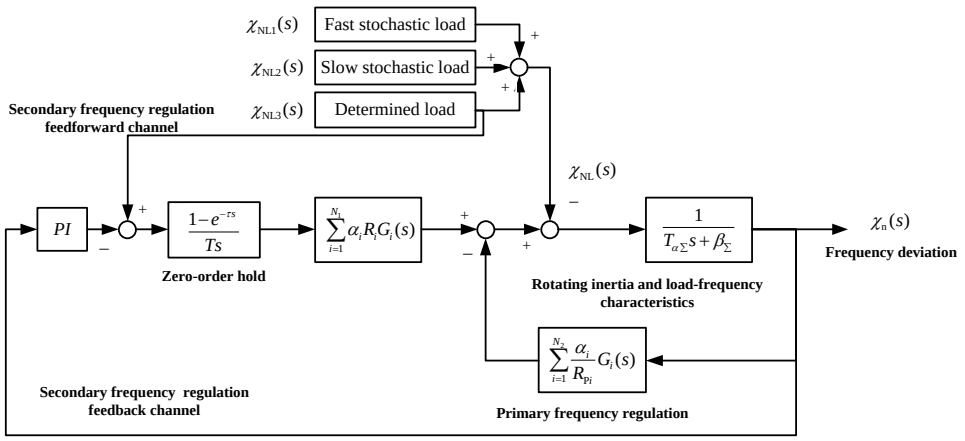

Fig. 4. *Frequency regulation model of a regional power system including air-cooled units*

3. The influence of direct air-cooled units on primary frequency regulation

3.1. Calculation of PFRA

There are many indexes to evaluate the operation performance of a power system, such as A1, A2, ACE, and the control performance standard CPS1 and CPS2 published by the North American Electric Reliability Council. However, these indexes could only measure the overall operation performance of the grid, not the grid's quick response ability when there are sudden accidents.

The primary frequency regulation ability (PFRA) is defined as the ratio of load change to frequency change of the grid only with the primary frequency regulation effect during a certain period of time. According to [17], PFRA can be calculated as:

$$PFRA=\sqrt{\left|\frac{\text{The variance of load deviation}}{\text{The variance of frequency deviation}}\right|} \tag{19}$$

Primary frequency regulation mainly deals with the fast stochastic load $\chi_{\mathrm{NL1}}(s)$. Thus, the relation between the grid's frequency deviation and load deviation can be expressed as:

$$\chi_{\mathrm{n}}(s)=H_1(s)\chi_{\mathrm{NL1}}(s) \tag{20}$$

where:

$$H_1(s)=-\frac{1}{T_{\alpha\Sigma}s+\beta_{\Sigma}+\sum_{i=1}^{N_2}\frac{\alpha_i}{R_{\mathrm{P}i}}G_i(s)} \tag{21}$$

Consider a linear system defined by its frequency response function $H(s)$, where $s=j\omega$. According to the Wiener-Khinchin theorem in [26-29], when the input signal $x(t)$ is a stochastic signal with an average value of zero, the variance of the output signal $y(t)$ can be expressed as:

$$\sigma_y^2=E\left\{y^2(t)\right\}=\frac{1}{2\pi}\int_{-\infty}^{+\infty}S_y(\omega)d\omega \tag{22}$$

where $S_y(\omega)$ is the power spectrum of output signal $y(t)$.

From [26-29], $S_y(\omega)$ is given by:

$$S_y(\omega)=S_x(\omega)\left|H(j\omega)\right|^2 \tag{23}$$

where $S_x(\omega)$ is the power spectrum of input signal $x(t)$.

Then, according to [30], any signal can be expressed as the convolution of impulse function $\delta(\mathrm{t})$ and the signal itself, and the power spectrum of $\delta(t)$ is equal to 1.

Thus, the variance of frequency deviation can be calculated by:

$$\begin{aligned}\sigma_{\chi_n}^2 &= \frac{1}{2\pi}\int_{-\infty}^{+\infty} S_\delta(\omega)\cdot\left|\chi_{\mathrm{NL1}}(j\omega)\right|^2\left|H_1(j\omega)\right|^2 d\omega \\ &= \frac{1}{2\pi}\int_{-\infty}^{+\infty} 1\cdot\left|\chi_{\mathrm{NL1}}(j\omega)\right|^2\left|H_1(j\omega)\right|^2 d\omega \\ &= \frac{1}{2\pi}\int_{-\infty}^{+\infty}\left|\chi_{\mathrm{NL1}}(j\omega)H_1(j\omega)\right|^2 d\omega\end{aligned} \tag{24}$$

By dividing $\sigma_{\chi_{\mathrm{NL1}}}^2$ by equation (24), it can be obtained that:

$$\frac{\sigma_{\chi_{\mathrm{NL1}}}^2}{\sigma_{\chi_n}^2} = \frac{\frac{1}{2\pi}\int_{-\infty}^{+\infty}\left|\chi_{\mathrm{NL1}}(j\omega)\right|^2 d\omega}{\frac{1}{2\pi}\int_{-\infty}^{+\infty}\left|\chi_{\mathrm{NL1}}(j\omega)H_1(j\omega)\right|^2 d\omega} \tag{25}$$

where $\sigma_{\chi_{\mathrm{NL1}}}^2$ is the variance of fast stochastic load.

To obtain the analytical expression of PFRA, more transformation is needed. According to the spectral characteristic of the ultra-short-term load, the load function is a limit power function. The high frequency component takes a small proportion, while the low frequency component takes a large one. Thus, the load frequency characteristic can be expressed as:

$$\chi_{\mathrm{NL}}(j\omega) = k\cdot W(j\omega) \tag{26}$$

where k is the amplitude of load deviation; $W(j\omega)$ is a shape function representing the distribution of load in frequency domain, which can be divided into the distribution function of the fast stochastic load , $W_1(j\omega)$, and the function of slow stochastic load , $W_2(j\omega)$.

Similarly, the fast stochastic load characteristic is given by:

$$\chi_{\mathrm{NL1}}(j\omega) = k_1\cdot W_1(j\omega) \tag{27}$$

where k_1 is the amplitude of fast stochastic load deviation.

Then, $\sigma_{\chi_{\mathrm{NL1}}}^2$ can be expressed as:

$$\sigma_{\chi_{\mathrm{NL1}}}^2 = \frac{1}{2\pi}\int_{-\infty}^{+\infty}\left|\chi_{\mathrm{NL1}}(j\omega)\right|^2 d\omega = \frac{1}{2\pi}\int_{-\infty}^{+\infty}\left|k_1 W_1(j\omega)\right|^2 d\omega = \frac{k_1^2}{2\pi}\int_{-\infty}^{+\infty}\left|W_1(j\omega)\right|^2 d\omega \tag{28}$$

Let k_1 be:

$$k_1 = \sqrt{2\pi}\sigma_{\chi_{\mathrm{NL1}}} \tag{29}$$

Then, $W_1(j\omega)$ satisfies:

$$\int_{-\infty}^{+\infty}\left|W_1(j\omega)\right|^2 d\omega = 1 \tag{30}$$

Then, equation (25) can be expressed as:

$$\begin{aligned}\frac{\sigma_{\chi_{\mathrm{NL1}}}^2}{\sigma_{\chi_{\mathrm{n}}}^2}&=\frac{\frac{1}{2\pi}\int_{-\infty}^{+\infty}\left|k_1W_1(j\omega)\right|^2d\omega}{\frac{1}{2\pi}\int_{-\infty}^{+\infty}\left|k_1W_1(j\omega)H_1(j\omega)\right|^2d\omega}=\frac{k_1^2\int_{-\infty}^{+\infty}\left|W_1(j\omega)\right|^2d\omega}{k_1^2\int_{-\infty}^{+\infty}\left|W_1(j\omega)H_1(j\omega)\right|^2d\omega}\\&=\frac{\int_{-\infty}^{+\infty}\left|W_1(j\omega)\right|^2d\omega}{\int_{-\infty}^{+\infty}\left|W_1(j\omega)H_1(j\omega)\right|^2d\omega}=\left|1\Big/\int_{-\infty}^{+\infty}\left|W_1(j\omega)H_1(j\omega)\right|^2d\omega\right|\end{aligned}\tag{31}$$

$W_1(j\omega)$ can be obtained from load characteristics modelling. $x_{\mathrm{NL1}}(t)$ represents the fast stochastic component in load, which reflects the randomness of load change. Thus, $x_{\mathrm{NL1}}(t)$ is a stationary time series and could be expressed by a second order autoregressive model:

$$x_{\mathrm{NL1}}(t)=\psi_1x_{\mathrm{NL1}}(t-\Delta t)+\psi_2x_{\mathrm{NL1}}(t-2\Delta t)+e_{\mathrm{t}}\tag{32}$$

where Δt is equal to 15 min; ψ_1 and ψ_2 are regression coefficients; and e_{t} is the white noise.

The corresponding $W_1(j\omega)$ could be calculated by equation (32) as long as the typical load data of a regional power grid is obtained. Thus, PFRA can be calculated by:

$$PFRA=\sqrt{\sigma_{\chi_{\mathrm{NL1}}}^2\Big/\sigma_{\chi_{\mathrm{n}}}^2}\tag{33}$$

The expression indicates the influence of the inertia time constant of the grid $T_{\alpha\Sigma}$ and the dynamic lag of the prime mover on PFRA.

3.2. The influence of meteorological conditions on PFRA

The two main meteorological conditions considered in this section are cooling air face velocity and the ambient temperature. The ratio of power units participating in primary frequency regulation is 50%，including 40% of air-cooled thermal units and 10% of hydro-power units. Parameter values of model in Fig.4 used for simulation are given in Table 4 [17].

To quantitatively measure the influence of cooling air face velocity and the ambient temperature on PFRA, the ambient temperature is supposed to remain unchanged at 40℃ and the values of PFRA under different face velocity conditions are calculated. Then, the cooling air face velocity is set at 2m/s and PFRA under different temperature conditions are calculated. The results are shown in Table 5 and Table 6.

Table 4 Parameter values of model in Fig.4

Parameters	Values
Ratio of installed capacity of air-cooled thermal units α_1	0.4
Ratio of installed capacity of hydro units α_2	0.1
Speed droop coefficient of air-cooled thermal units R_{P1}	0.05
Speed droop coefficient of hydro generators units R_{P2}	0.04
Inertia time constant of electric power system $T_{\alpha\Sigma}$	8s
Load-frequency characteristic coefficient β_{Σ}	1.6
Control cycle of secondary frequency regulation T	15s
Proportional parameter of PI controller	0.25
Integral parameter of PI controller	1
Coefficient of power budget of air-cooled units in secondary frequency regulation R_1	0
Coefficient of power budget of hydro units in secondary frequency regulation R_2	0
Permanent speed droop coefficient b_p	0.04
Proportional parameter of PID controller K_P	5.185
Integral parameter of PID controller K_I	0.988
Differential parameter of PID controller K_D	3.333
Inertia time constant of hydro units T_w	1.5s
Hydraulic servo-motor time constant T_{ws}	0.2s
Pilot valve time constant T_σ	0.03s

Table 5 PFRA under different air face velocity conditions

Cooling air face velocity/(m/s)	PFRA
2	55.5762
3	58.3814
4	59.3505
5	59.946
6	60.5677
7	61.3353
8	62.1308

Table 6 PFRA under different temperature conditions

Ambient temperature/℃	PFRA
20	59.9138
25	58.9095
30	57.9688
35	56.8899
40	55.5762

From Table 5, PFRA decreases as the air face velocity decreases. When the face velocity decreases from 8m/s to 3m/s, the value of PFRA decreases by 0.8 on average as face velocity drops 1m/s. When the face velocity decreases from 3m/s to 2m/s, PFRA decreases by 2.8, which is the highest difference value occurred in 1 m/s interval.

From Table 6, PFRA decreases as the ambient temperature rises. PFRA decreases by 1 as temperature drops 5℃ when the ambient temperature rises from 20℃ to 35℃. When the ambient temperature rises from 35℃ to 40℃, PFRA decreases by 1.3, which is the highest difference value occurred in 5℃ interval.

Thus, the relations between PFRA and meteorological conditions are nonlinear. By Matlab curve fitting, the relations can be expressed respectively as:

$$PFRA = -0.00103v^6 + 0.0343v^5 - 0.478v^4 + 3.586v^3 - 15.285v^2 + 35.614v + 23.417 \quad (34)$$

$$PFRA = 7.013\times10^{-6}t_a{}^4 - 0.001041t_a{}^3 + 0.052837t_a{}^2 - 1.315t_a + 72.285 \quad (35)$$

The corresponding plots are shown in Fig.5.

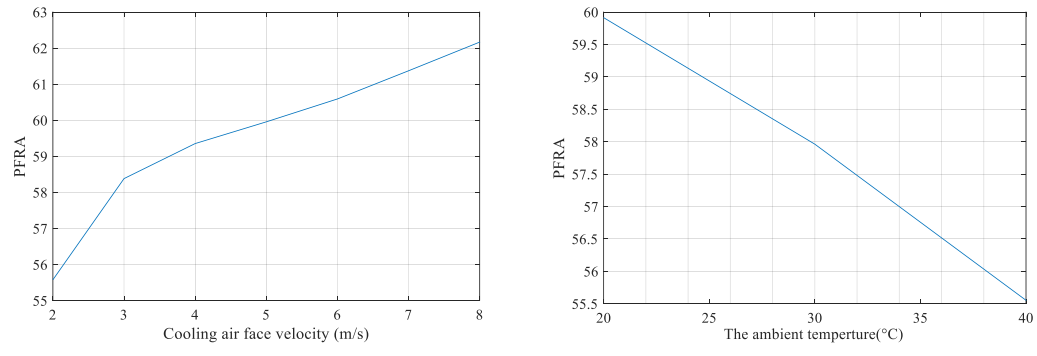

a *b*

Fig.5. *Relations between PFRA and meteorological conditions*
a PFRA under different cooling air face velocity conditions
b PFRA under different ambient temperature conditions

PFRA is also analysed in frequency domain, which is shown in Fig.6.

The decrease of cooling air face velocity or the increase of the ambient temperature results in the decrease in the amplitude of $\chi_{\mathrm{n}}(s)/\chi_{\mathrm{NL1}}(s)$ and the increase of the phase margin. The variations of amplitude and phase margin are non-linear, which are consistent with the previous analysis.

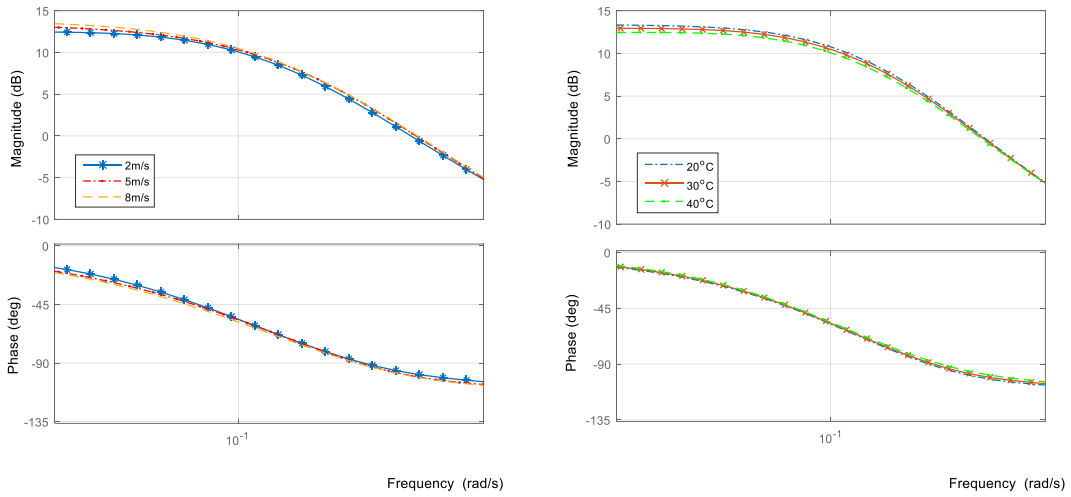

a *b*

Fig.6. *Frequency-response characteristics under different meteorological conditions*
a Frequency-response characteristics under different cooling air face velocity conditions
b Frequency-response characteristics under different ambient temperature conditions

4. Case study

From previous analysis, a high ambient temperature and a low cooling air face velocity can restrict the generating ability of an air-cooled unit. The ambient temperature is set at 40℃ and the face velocity of the cooling air is 2m/s, which is a disadvantageous condition for air-cooled units.

In this section, cases under generator tripping and steep load rising conditions are studied. Air-cooled units included in this section are coal-fired reheating thermal power plants modelled in Section 2.2. The maximum proportions of air-cooled units allowed connecting to the grid and the corresponding PFRA are calculated under these conditions.

4.1. Case A: generator tripping case

In this case, one unit suddenly comes off the grid at 10s. Responses of the grid with different proportions of air-cooled units are studied. The simulation results are shown in Fig.7.

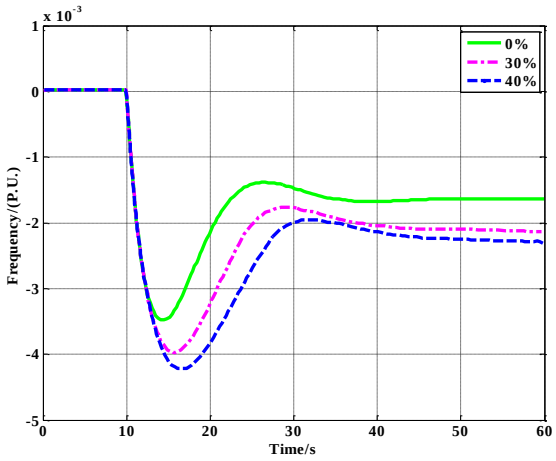

Fig.7. *Responses of a gird with different ratio of air-cooled units after one unit comes off*

From the simulation results, the frequency overshoot and regulation time increase as the proportion of air-cooled units rises. The frequency deviation is supposed to be kept within 0.2Hz, which is 0.004p.u. When the proportion reaches 30%, the frequency deviation just critically meets the requirement, which means the maximum proportion of air-cooled units should be kept within 30% under this condition. The corresponding PFRA is 57.3994.

4.2. Case B: steep load rising case

In this case, load steeply rises at 10s. Responses of the grid with different proportions of air-cooled units are studied, as shown in Fig.8.

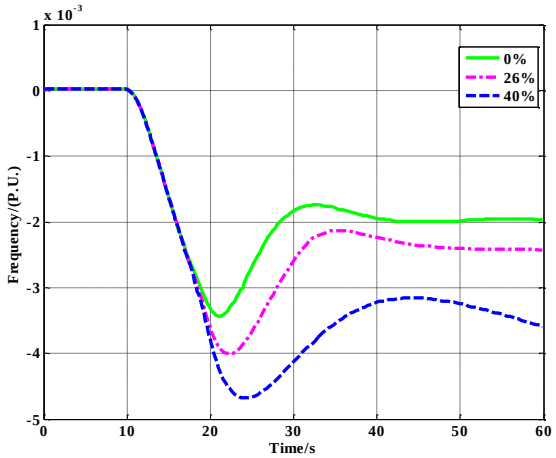

Fig.8. *Responses of a grid with different proportions of air-cooled units after a steep load rise*

The frequency overshoot and regulation time increase as the power proportion of air-cooled units rises. When the proportion of air-cooled units reaches 26%, the frequency deviation just critically meets the requirements. The corresponding PFRA is 58.1256.

These cases provide examples to determine the maximum proportion of air-cooled units allowed in the grid under extreme conditions. These results would also be instructive for operation formulation of the grid.

5. Conclusions

Considering the impact of the ambient temperature and cooling air face velocity, a new model of air-cooled units is developed. Then, the primary frequency regulation process is studied based on the model of a regional grid including air-cooled units. A parameter is defined to quantitatively measure the primary frequency regulation ability of the grid. PFRA is calculated as the square root of the absolute specific value of the variance of load deviation to the variance of frequency deviation. The nonlinear mathematical formulas between PFRA and the meteorological parameters show that a high ambient temperature and a low cooling air face velocity restrict the grid's frequency regulation ability. This conclusion is also proved by simulations in frequency domain. Finally, the responses of a regional power grid under extreme conditions are simulated, where the maximum proportions of air-cooled units allowed under each condition and the corresponding PFRA are given. This model and simulation method is significative to practical operation and strategy formulation for power systems with air-cooled units under different meteorological conditions.

6. Acknowledgments

This work was financially supported by the National Natural Science Foundation of China (Grant No.51107014 and No.51676054).

7. References

[1] Liu, J., Hu, Y., Zeng, D., *et al*.: 'Optimization of an air-cooling system and its application to grid stability', Applied Thermal Engineering, 2013, **61**, (2), pp. 206-212

[2] Liu, L., Du, X., Xi, X., *et al*.: 'Experimental analysis of parameter influences on the performances of direct air cooled power generating unit', Energy, 2013, **56**, (56), pp. 117–123

[3] Zhang, Z., Yang, J., Wang, Y.: 'A favorable face velocity distribution and a v-frame cell for power plant air-cooled condensers', Applied Thermal Engineering, 2015, **87**, pp. 1-9

[4] Yang, L. J., Chen, L., Du, X. Z., *et al*.: 'Effects of ambient winds on the thermo-flow performances of indirect dry cooling system in a power plant', International Journal of Thermal Sciences, 2013, **64**, (2), pp. 178-187

[5] Mohapatra,A. K., Sanjay. : 'Analysis of parameters affecting the performance of gas turbines and combined cycle plants with vapor absorption inlet air cooling', International Journal of Energy Research, 2014, **38**, (38), pp.223–240

[6] Du, X., Hu, H., Shen, Y., *et al*.: 'Reduced order analysis of flow and heat transfer for air-cooled condenser of power generating unit ', Applied Thermal Engineering, 2013, **51**, (s 1–2), pp. 383–392

[7]Dong, S., Liu, J.: 'Simulation analysis and mathematics model study of direct air-cooling condenser', IEEE International Conference on Automation and Logistics, Qingdao, China, SEP 2008, pp. 2843-2846

[8] Bracco, S., O. Caligaris, A. Trucco.: 'Mathematical models of air-cooled condensers for thermoelectric units', WIT Transactions on Ecology and the Environment, 2009, **121**, (2), pp. 389-400

[9] Du, X., Liu, L., Xi, X., *et al*.: 'Back pressure prediction of the direct air cooled power generating unit using the artificial neural network model', Applied Thermal Engineering, 2011, **31**, (14), pp. 3009-3014

[10] Al-Mutairi, E. M., Odejobi, O. J.: 'Investigating the thermodynamics and economics of operating the thermal power plant under uncertain conditions ', Energy Conversion & Management, 2013, **75**, (5), pp. 325-335

[11] Guo, W., Tang, Y., Dai, Y., *et al*.: 'The Analysis of the Primary Frequency Regulation in Electric Power System', International Forum on Energy, Environment and Sustainable Development, Shenzhen, China, APR 2016, pp. 1117-1121

[12] Dai, Y., Xu, Y., Dong, Z. Y., *et al*.: 'Real-time prediction of event-driven load shedding for frequency stability enhancement of power systems', IET Gener. Transm. Distrib., 2012, **6**, (9), pp. 914-921

[13] Prasad, S., Purwar, S., Kishor, N.: 'H -infinity based non-linear sliding mode controller for frequency regulation in interconnected power systems with constant and time-varying delays ', IET Gener. Transm. Distrib., 2016, **10**, (11), pp. 2771-2784

[14] Vidyanandan, K. V., Senroy, N.: 'Frequency regulation in a wind–diesel powered microgrid using flywheels and fuel cells ', IET Gener. Transm. Distrib., 2016, **10**, (3), pp. 780-788

[15] Dai, J., Phulpin, Y., Sarlette, A., *et al*.: 'Coordinated primary frequency control among non-synchronous systems connected by a multi-terminal high-voltage direct current grid', IET Gener. Transm. Distrib., 2012, **6**, (2), pp. 99-108

[16] Bevrani, H., Ledwich, G., Dong, Z. Y., *et al*.: 'Regional frequency response analysis under normal and emergency conditions', Electric Power Systems Research, 2009, **79**, (5), pp. 837-845

[17] Guo, Y., Zhao, X. M., Hong, L.: 'Boundaries of Power System Frequency Regulation Ability', Power and Energy Engineering Conference, Wuhan, China, MAR 2009, pp.1-4

[18] Zhang,X., Chen, H.: 'Performance Forecast of Air-Cooled Steam Condenser under Windy Conditions', Journal of Energy Engineering, 2015, **142**, (1), pp. 04015010 1-15

[19] Yang, L. J., Du, X. Z., Yang, Y. P.: 'Space characteristics of the thermal performance for air-cooled condensers at ambient winds ', International Journal of Heat & Mass Transfer, 2011, **54**, (15), pp. 3109-3119

[20] Xiao, L., Ge, Z., Du, X., *et al*.: 'Operation of air-cooling chp generating unit under the effect of natural wind', Applied Thermal Engineering, 2016, **107**, pp. 827-836

[21] Larinoff, M. W., Moles, W. E., Reichhelm, R.: 'Design and specification of air-cooled steam condensers ', Chemical Engineering, 1978, **85**, (12), pp. 86-94

[22] Walraven, D., Laenen, B., D'Haeseleer, W.: 'Minimizing the levelized cost of electricity production from low-temperature geothermal heat sources with ORCs: Water or air cooled? ', Applied Energy, 2015, **142**, pp. 144-153

[23] Bari, E., Noel, J. Y., Comini, G., *et al*.: 'Air-cooled condensing systems for home and industrial appliances', Applied Thermal Engineering, 2005, **25**, (10), pp. 1446-1458

[24] Guo, Y., Yu, D.: ' The influence of interconnection of electric power systems on load characteristic and frequency regulation', Electric Power Systems Research, 2004, **70**, (1), pp. 23-29

[25] Group, W.: 'Hydraulic turbine and turbine control models for system dynamic studies ', IEEE Transactions on Power Systems, 2002, **7**, (1), pp. 167-179

[26] Papoulis, A., and Pillai, S.U.: 'Probability, Random Variables and Stochastic Processes' (McGraw-Hill Education, New York, 2002, 4th edn. 2012)

[27] Peyton, Z., Peebles, Jr.: 'Probability, Random Variables, and Random Signal Principles'(McGraw-Hill Education, New York, 1980, 2nd edn. 1987)

[28]James, V.C. : 'Signal Processing: The Model-Based Approach '(McGraw-Hill Education, New York, 1986, 1st edn. 1986)

[29]Sophocles, J.O. : 'Optimum Signal Processing: An Introduction'(Macmillan,New York, 1985,2nd edn. 1988)

[30]Gordon, E. C. : 'Signal and Linear System Analysis' (John Wiley & Sons, Inc., New York, 1995, 1st edn. 1995)